International Journal of Engineering Research & Technology (IJERT)
ISSN: 2278-0181
Vol. 4 Issue 04, April-2015

Comparitive Study of Astronomical Image Denoising Using Richardson Lucy Deconvolution Algorithm With Wavelet Thresholding

Prof. Rishidas. S
Associate prof,Dept of AEI
Govt Engineering College,
Kozhikode, India

Rolitta V Babu
Dept of Electronics
Govt Engineering College
Kozhikode

Prof. Sujith Kumar T P
Assistant Professor
Dept of Electronics
Govt Engineering College
Kozhikode.

***Abstract*—Denoising astronomical images which is corrupted by huge sources of celestial and atmospheric noises is a field of great importance. Richardson Lucy deconvolution is a conventional method that is used for this denoising. In this paper we have implemented this Richardson Lucy deconvolution algorithm after a preprocessing. Here we adopted wavelet domain preprocessing. Methods adopted for that include thresholding at wavelet domain and Gabor filtering.**

I. ASTRONOMICAL IMAGES

Astronomical images are taken and saved at different conditions using various method. In the physical sciences almost all signals is affected by noise, and noise removal is therefore a useful preliminary for interpretation of data and to extract useful information from it through various image processing tools.We need to bypass instrumental measurement artifacts too.

CCD camera is mainly used to capture astronomical images. Also high resolution DSLR cameras are used. Astronomical images captured using such camera suffers from severe noise effects. Noisy image we collected may be unacceptable for analysis and observation. Noise may be due to the instrumental misalignments or due to atmospheric disturbances. Astronomical images differ from other images due to several unique characteristics like they are distant images, most images are with dark background, faint object, may contain point objects, angular dimension is small. Denoising them is a matter of great importance. It contains data encapsulated in large amount of noises. Wide sources of noise are present. **Noise** from different atmospheric layers (turbulence), sensor generated noise, noise created by sun and other extra terrestrial objects. The atmospheric turbulence blur degrades images by many ways like, images taken by cameras viewing scenes from long distances, The earth turbulent atmosphere, long exposure imaging due to a low illumination environment, [1] and dust particles on the surface of the lens are the main reason for the blur to happen

II. DENOISING ASTRONOMICAL IMAGES

In this paper we are trying to denoise the astronomical images using conventionally implemented Richardson Lucy deconvolution algorithm [2] with some pre-processing applied to the noisy image. A result comparison is done in terms of PSNR value, Image Enhancement Factor [6] and structural similarity (SSIM) [7]. Adequate noise is added to observe the result. Images for the experiments are collected by means of a high resolution camera at various conditions of sky.

A. *Richardson Lucy Deconvolution Algorithm*

Richardson Lucy is a deconvolution [4], [5] algorithm which is an existing method widely used for denoising the astronomical images. The Richardson–Lucy algorithm, also known as Lucy–Richardson deconvolution, is an iterative procedure for recovering a latent image that has been blurred by a known point spread function. It got its name after William Richardson and Leon Lucy, who defined it independently.

Main idea of deconvolution comes from finding a degradation function PSF and then convolving the obtained degraded image with the inverse PSF. In this case as the image is recorded on a detector such as photographic film or a Charge-Coupled device, it will be degraded. That is ideal point sorcr will be spread out to a Point Spread Function.

Non-point sources are effectively the sum of many individual point sources, and pixels in an observed image can be represented in terms of the point spread function and the latent image as

$$di = \sum p(i,j)u(j) \qquad (1)$$

p is the point spread function, u(j) is the pixel value at location j in the latent image, and di is the observed value at pixel location i. The basic idea is to calculate the most likely u(j) given the observed di and known p(i,j). This leads to an equation for u(j) which can be solved iteratively according to

$$u_j^{(t+1)} = u_j^{(t)} \sum_i \frac{d_i}{c_i} p_{ij} \qquad (2)$$

Where $$c_i = \sum_j p_{ij} u_j^{(t)} \qquad (3)$$

Block diagram of the implemented system

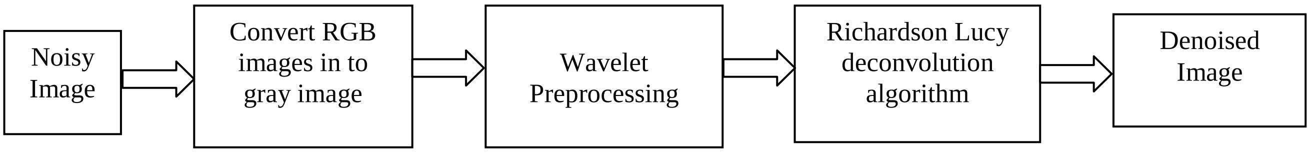

It has been shown empirically that if this iteration converges, it converges to the maximum likelihood solution for u(j) [11]. This can also be written more generally (for more dimensions) in terms of convolution [10],

$$u^{(t+1)} = u^{(t)} \cdot \left(\frac{d}{u^{(t)} \otimes p} \otimes \hat{p} \right) \quad (4)$$

Here we are assuming a Gaussian PSF.

PSF is an important parameter that decides the quality of restored image. PSF has to be found by optimizing using Expectation Maximization algorithm which yet has to be incorporated to the currently implemented algorithm.

Thresholding

A Wavelet is a waveform of efficiently limited duration that has no average value zero. Transforming the image into wavelet doman will produce corresponding 4 subbands. Donoho and Johnston proposed hard and soft thresholding methods for denoising. Threshold for each subband is determined and applied according to the type of thresholding scheme. This method eliminates many wavelet coefficients that might contain useful image information. However, the major problem with both methods is the choice of a suitable threshold value. Many wavelet based thresholding techniques like Visu shrink, Oracle Shrink, Normal shrink have proved better efficiency in image denoising [12].

B. Hard thresholding

I. Take the wavelet transform. (Daubechies, Haar)
II. Find the suitable threshold for each subband.
   - Adaptive threshold selection using principle of Stein's Unbiased Risk Estimate.
   - Minimax thresholding.
III. If H(i,j) < threshold , then H(i,j) =0

C. Soft Thresholding

I. Repeat first two steps of hard thresholding.
II. D(U,T) = sgn(U)max(0,|U|-T)

D. Gabor filtering

The Gabor function has been used as an efficient representation of two dimensional signals. The Gabor filters have received considerable attention in the computer vision field since the characteristics of certain cells in the visual cortex of some mammals can be approximated by these filters. They realize multichannel filtering which decompose an input image into a number of filtered images. Each filtered image contain intensity variation over a narrow range of frequency and orientation [13].

Two dimensional Gabor filter is given as a product of a 2D Gaussian function and a plane wave propagating to some direction on 2D plane. It is determined by the standard deviation of the Gaussian function and the propagating direction and the wave length of the plane wave. Since the standard deviation rules the extent of a Gaussian function, it also rules that of the Gabor filter. Thus the standard deviation is closely related to the wave length of a plane wave. The 2D Gabor filter is defined as a complex function, and its real and imaginary part are used as two real filters. The following equations show 2D Gabor filters.

$$R(x,y;\nu,k) = \exp(-\frac{x^2+y^2}{2\sigma_\nu^2}) \cdot \cos\frac{\pi}{\sigma_\nu}(x\cos\phi_k + \sin\phi_k) \quad (5)$$

$$I(x,y;\nu,k) = \exp(-\frac{x^2+y^2}{2\sigma_\nu^2}) \cdot \sin\frac{\pi}{\sigma_\nu}(x\cos\phi_k + \sin\phi_k) \quad (6)$$

$$\sigma_\nu = (\sqrt{2})^{\nu+1} \quad (7)$$

$$\phi_k = \frac{\pi}{4}k \quad (8)$$

Appropriate values are given to v and k to get the Gabor filters that maximizes our performance. R and I are convolved with our noisy image to have the filter responses. These subbands are then thresholded before reconstruction.

B. Performance Measures

(a) PSNR

Peak signal to noise ratio is calculated [6]. The formula for PSNR is

$$PSNR = 10*10\log 10(\frac{255^2}{MSE}) \quad (7)$$

$$MSE = \sum_{m,n} \frac{[(O(m,n) - R(m,n))^2]}{(M*N)} \quad (8)$$

Where *MSE* means Mean Square error. *O* is the original image, *R* is the restored image, *P* is the corrupted image and MXN is the size of the original input image.

(b) IEF

Image Enhancement Factor is another performance measure that is calculated from the following expression.

$$IEF = \left(\sum_{m,n}(P(m,n)-O(m,n))^2\right) \Big/ \left(\sum_{m,n}(R(m,n)-O(m,n))^2\right) \quad (9)$$

(c) SSIM (structural similarity)

This is a quality assessment method that take advantage of known characteristics of the human visual system (HVS). structural similarity (SSIM) that compares local patterns of pixel intensities that have been normalized for luminance and contrast.

The local statistics are computed within a local 8X8 square window, which moves pixel-by-pixel over the entire image. At each step, the local statistics and SSIM index are calculated within the local window. Similarity is measured from SSIM index. Various formulas and parameters are needed for SSIM calculation [7].

III. EXPERIMENTAL OBSERVATIONS

Some of the observations are shown below. Fig (a) to fig (j). Several celestial images are processed. Here we have given two of them for the comparative study. Image set includes Jupiter planet and its associated moons and lunar image those are collected by a high resolution camera.

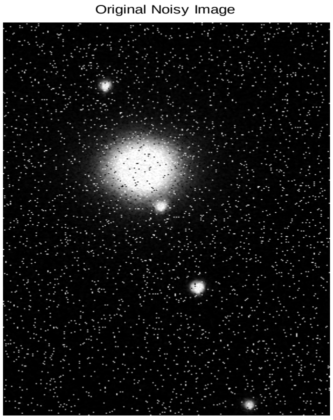

(a)

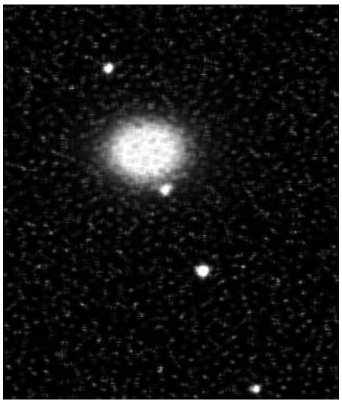

(b)

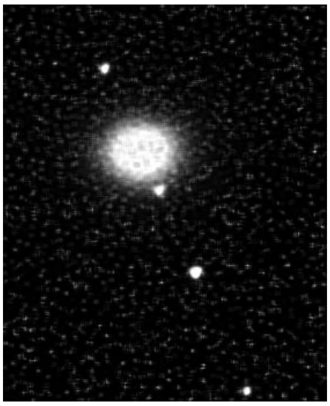

(c)

(d)

(a) Jupiter-Original image in clear sky, (b) Restored image using Richardson Lucy Deconvolution (c) Restored image with hard thresholding Preprocessing Image with Gabor filtering thresholding Preprocessing

ISSN: 2278-0181
Vol. 4 Issue 04, April-2015

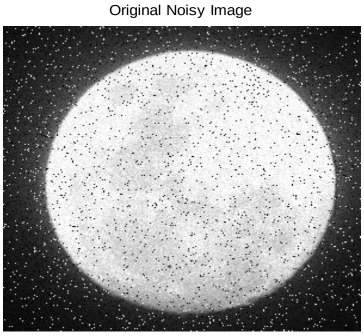

(e)

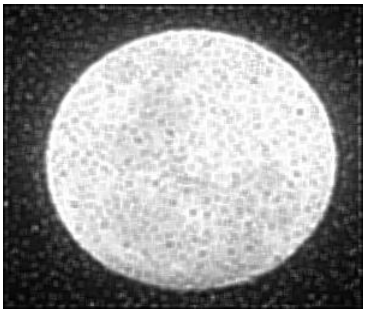

(f)

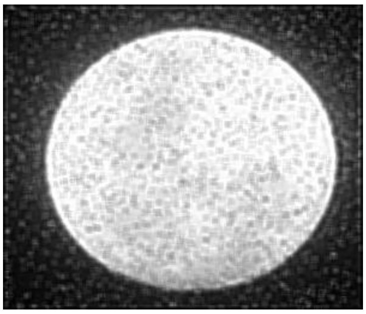

(g)

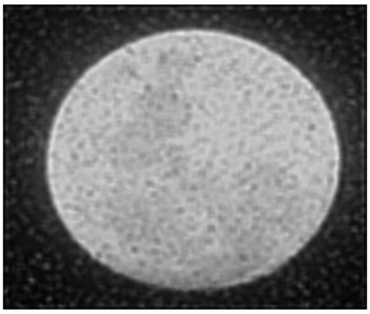

(h)

(e) Lunar-Original image (f) Restored image using Richardson Lucy Deconvolution (g) Restored image with soft thresholding Preprocessing (h) Restored Image with Gabor filtering thresholding

TABLE I. ANALYSIS OF RESTORED IMAGES

Image	Restoration Method	Performance Measures					
		No: Iterations	*Time of Iteration*	*PSNR*	*RMSE*	*IEF*	*MSSIN*
Jupiter and its satellites-Clear sky	RL Algorithm	4	1.73858	24.901	14.19414	7.4984	0.433267
	Hard Thresholding	4	6.449743	24.5939	14.91262	6.9321	0.426753
	Soft Thresholding	4	1.55833	24.8757	14.25821	7.4497	0.431767
	Gabor Filter Preprocessing	4	1.49657	25.2443	13.71133	8.152	0.530491
Lunar Image	RL Algorithm	4	1.08172	23.9706	16.1977	5.3994	0.45348
	Hard Thresholding	4	1.5674	23.9962	15.82676	5.4042	0.452234
	Soft Thresholding	4	0.463241	24.0597	16.23008	5.654	0.463241
	Gabor Filter Preprocessing	4	1.5576	14.5759	43.69724	0.7361	0.613426

Here thresholding is done at three level Daubechies discrete wavelet transform. From various analyses we can infer many things. Apart from these two images, we also analyzed about 20 different images for theses four sets of algorithms. By observing different performance measures we can say that any of the preprocessing with Richardson Lucy deconvolution algorithm cannot improve the denoised image quality.

While comparing different preprocessing techniques we cannot say that best results are obtained for particular preprocessing. But one thing we can say is that soft thresholding is better than hard thresholding. Here we considered two different thresholding schemes. The result shown is obtained by using universal threshold, which gives a better performance comparatively for this application.

While comparing the performance measures we can see that thresholding not always improves the image quality. This is because of the particular properties of astronomical images. Due to thresholding we are losing some important data. In the case of hard thresholding sometimes pure noise coefficients may pass the hard threshold and appear as annoying 'blips' in the output. We expect soft threshold will avoid this. That is the reason for a bit improvement in PSNR while compared with hard threshold. About 0.3db change is observed. Gabor filtering thresholding has shown improved performance for point object images. But inferior at the case of surface images (lunar image, 14.5759 db).

Here we are trying to eliminate high frequency artifacts and this result in a blurring effect at the output. The restoration process in the situation of the existence of blur and noise combined together is complicated. Unfortunately, in this situation when trying to restore a blurry and noisy image, the effect will be adverse.

IV. CONCLUSION

From the observations we can see a bit improvement in performance while preprocessing. Also corresponding change is observed in all other parameters. Improvement not only depends on the processing method, but also the image properties.

In the result we can see there still exists a hallow around the objects which is the result of atmospheric turbulence and the image is blurred as a consequence of noise removal. Noise is not always Gaussian. It may be Poisson or combinations of Poisson and Gaussian. So atmospheric noise modeling is required. Atmospheric modeling may give better PSF and thus improve the deconvolution. As a part of future work we are trying to incorporate the Expectation Maximization algorithm for this modeling.

REFERENCES

1. Zohair Al-Ameen, DzulkifliMohamad, MohdShafry M.R and GhazaliSulong ."Restoring Degraded Astronomy Images using a Combination of Denoising and Deblurring Techniques".International Journal of Signal Processing, Image Processing and Pattern Recognition. Vol. 5, No. 1, March, 2012
2. J. L. Starck and E. Pantin. "Deconvolution in Astronomy: A Review". Publications of the Astronomical Society of the Pacific, 114:1051–1069, 2002 October 2002. The Astronomical Society of the Pacific.
3. "Astronomical Image Processing A1". Imperial College London Publication.
4. William Hadley Richardson "Bayesian-Based Iterative Method of Image Restoration". Journal Of The Optical Society Of America. Volume 62, Number I. January 1972
5. L.B. Lucy. An iteration technique for the rectification of observed distributions.Astronomical Journal, 79:745–754, 1974.
6. Jean-Luc Starck and FionnMurtagh, "Handbook of Astronomical Data Analysis".
7. SruthiIgnatious . International Journal Of Engineering And Computer Science ISSN:2319-7242 Volume - 3 Issue -9 September, 2014 . "Removal of High Density Salt and Pepper Noise from Digital Images".
8. Zhou Wang. " Image Quality Assessment: From Error Visibility to Structural Similarity". IEEE Transactions On Image Processing, Vol. 13, No. 4, April 2004
9. Dilip Krishnan, Terence Tay, Rob Fergus. "Blind Deconvolution Using a Normalized Sparsity Measure".
10. Scott S. Sheppard & David C. Jewitt, "An abundant population of smallirregular satellites around Jupiter." Institute for Astronomy, University of Hawaii, 2680 Woodlawn Drive, Honolulu,Hawaii 96822, USA.
11. Fish D. A.,; Brinicombe A. M., Pike E. R., and Walker J. G. (1995), "Blind deconvolution by means of the Richardson–Lucy algorithm", Journal of the Optical Society of America A 12 (1): 58–65, Bibcode:1995JOSAA..12...58F, doi:10.1364/JOSAA.12.000058
12. Shepp, L. A.; Vardi, Y. (1982), "Maximum Likelihood Reconstruction for Emission Tomography", IEEE Transactions on Medical Imaging 1:13,doi:10.1109/TMI.1982.4307558
13. Rajesh Kumar Rai, Trimbak R. Sontakke, "Implementation of Image Denoising using Thresholding Techniques", International Journal of Computer Technology and Electronics Engineering (IJCTEE) Volume 1 , Issue 2.
14. *Shinji Umeyama*, "Blind Deconvolution Of Images Using Gabor Filters And Independent Component Analysis", 4th International Symposium On Independent Component Analysis And Blind Signal Separation (Ica2003), April 2003, Nara, Japans